Supporting Information to

Open circuit voltage and efficiency in ternary organic photovoltaic blends

Nikolaos Felekidis[1], Ergang Wang[2], Martijn Kemerink[1,3]

[1] Complex Materials and Devices, Department of Physics, Chemistry and Biology (IFM), Linköping University, SE-581 83 Linköping, Sweden

[2] Department of Chemistry and Chemical Engineering, Chalmers University of Technology, SE-412 96 Göteborg, Sweden

[3] Department of Applied Physics, Eindhoven University of Technology, PO Box 513, NL-5600 MB Eindhoven, The Netherlands
E-mail: martijn.kemerink@liu.se

Contents

1 – Chemical structure and full compound names

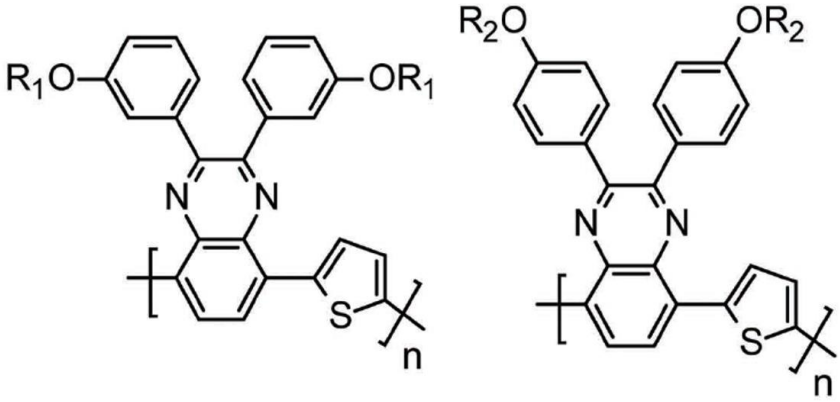

TQ_{m6} R_1 = n-C_6H_{13}
TQ_{m12} R_1 = n-$C_{12}H_{25}$

TQ_{p6} R_2 = n-C_6H_{13}

Fig. S1. Molecular structure of TQm6,TQm12 and TQp6.

Poly[2,3-bis-(3-hexyloxyphenyl)quinoxaline-5,8-diyl-alt-thiophene-2,5-diyl] (**TQm6**)

Poly[2,3-bis-(3-dodecyloxyphenyl)quinoxaline-5,8-diyl-alt-thiophene-2,5-diyl] (**TQm12**)

Poly[2,3-bis-(4-hexyloxyphenyl)quinoxaline-5,8-diyl-alt-thiophene-2,5-diyl] (**TQp6**)

2 – AFM images of film morphology

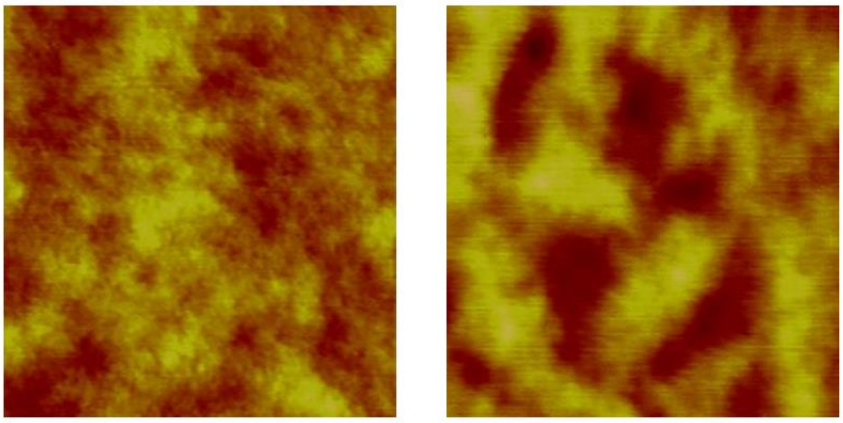

Fig. S2. AFM images of TQm6:TQm12:$PC_{71}BM$ BHJ OPV. The left (right) picture corresponds to TQm6/(TQm6+TQm12) = 0.5 (0.6). Scan size is 3×3 µm, total vertical scale is 10 nm.

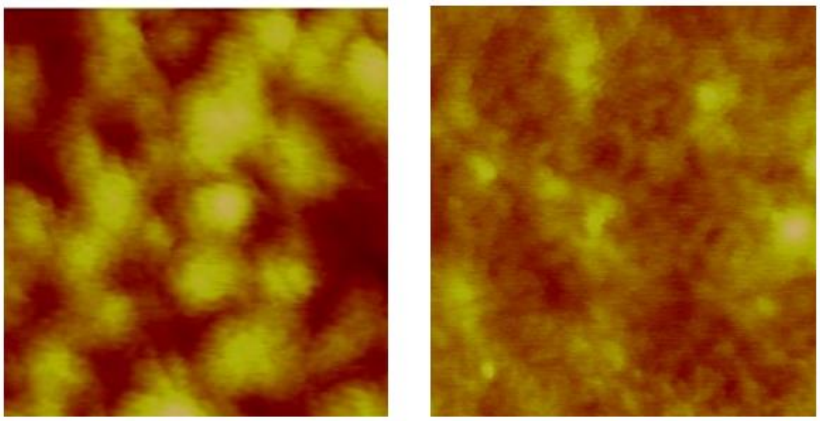

Fig. S3. AFM images of TQp6:TQm6:$PC_{71}BM$ BHJ OPV. The left (right) picture corresponds to TQp6/TQp6+TQm6 = 0.2 (0.6). Scan size is 3×3 µm, total vertical scale is 10 nm.

3 – Fill factors for TQx:TQy:$PC_{71}BM$

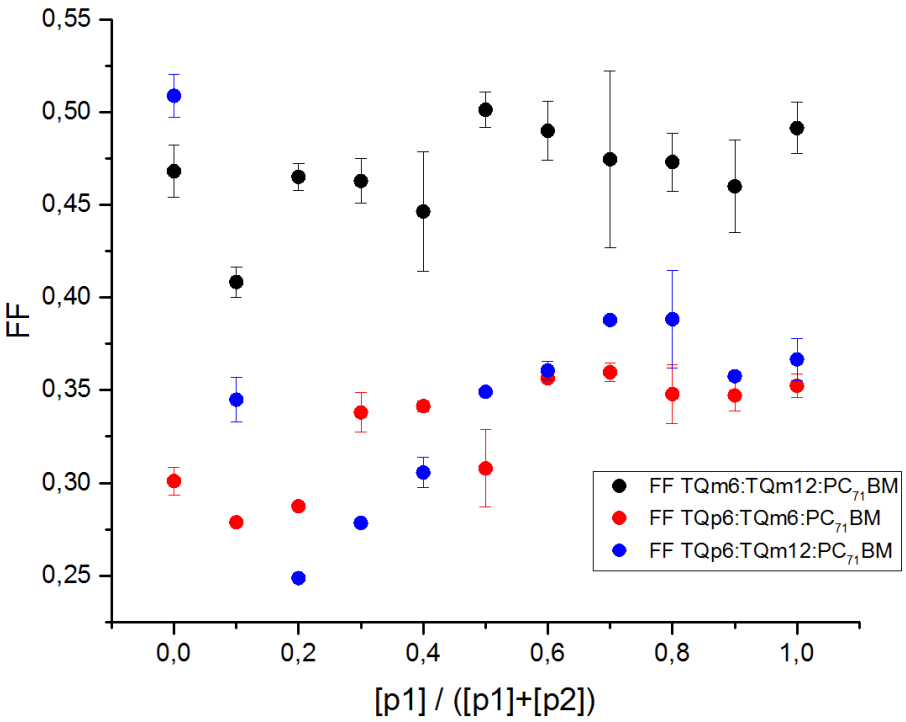

Fig. S4. Fill factors for all three TQx:TQy:$PC_{71}BM$ polymer combinations.

4 – Parameter values for Fig. 4

σ_{TQm6} [eV]	0.1	**σ_{TQp6} [eV]**	0.12
σ_{TQm12} [eV]	0.104	**σ_{TQm12} [eV]**	0.104
σ_{PC71BM} [eV]	0.12	**σ_{PC71BM} [eV]**	0.12
occupation	$1.05 \cdot 10^{-3}$	**occupation**	10^{-3}
DOS	10^{26}	**DOS**	10^{26}
HOMO $_{TQm6}$ [eV]	-5.72	**HOMO $_{TQp6}$ [eV]**	-5.55
HOMO $_{TQm12}$ [eV]	-5.76	**HOMO $_{TQm12}$ [eV]**	-5.76
LUMO $_{PC71BM}$ [eV]	-4.1	**LUMO $_{PC71BM}$ [eV]**	-4.1

Table S1. Parameter values used in the simulation model for the fitting of TQm6:TQm12:$PC_{71}BM$ and TQm6:TQm12:$PC_{71}BM$ assuming constant occupation.

5 – Fitting Voc for literature data

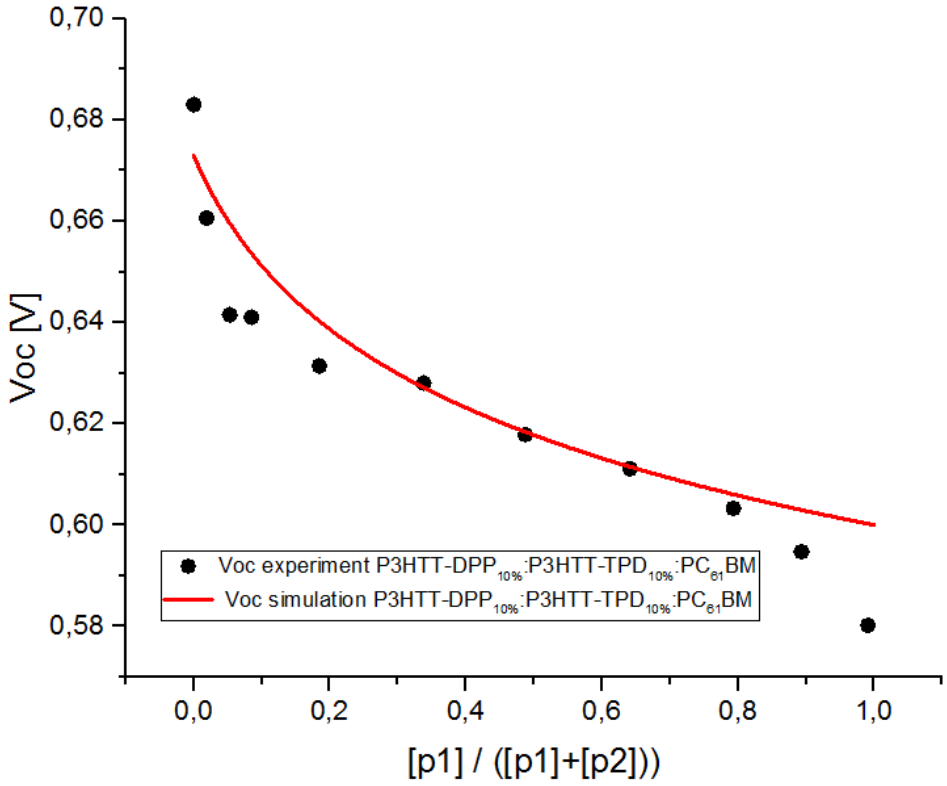

Fig. S5. Fitting of the P3HTT-DPP10%:P3HTT-TPD10%:PC61BM ternary BHJ OPV from Khlyabich *et al*. [1] assuming constant occupation.

σ P3HTT-DPP10% [eV]	0.075
σ P3HTT-TPD10% [eV]	0.105
σ PC61BM [eV]	0.075
occupation	$1.2 \cdot 10^{-3}$
total_Po_No	10^{26}
HOMO P3HTT-DPP10% [eV]	-5.25
HOMO P3HTT-TPD10% [eV]	-5.40
LUMO PC61BM [eV]	-4.10

Table S2. Parameter values used in the simulation model for the fitting of the P3HTT-DPP10%:P3HTT-TPD10%:PC61BM ternary BHJ OPV from Khlyabich *et al*. [1] assuming constant occupation.

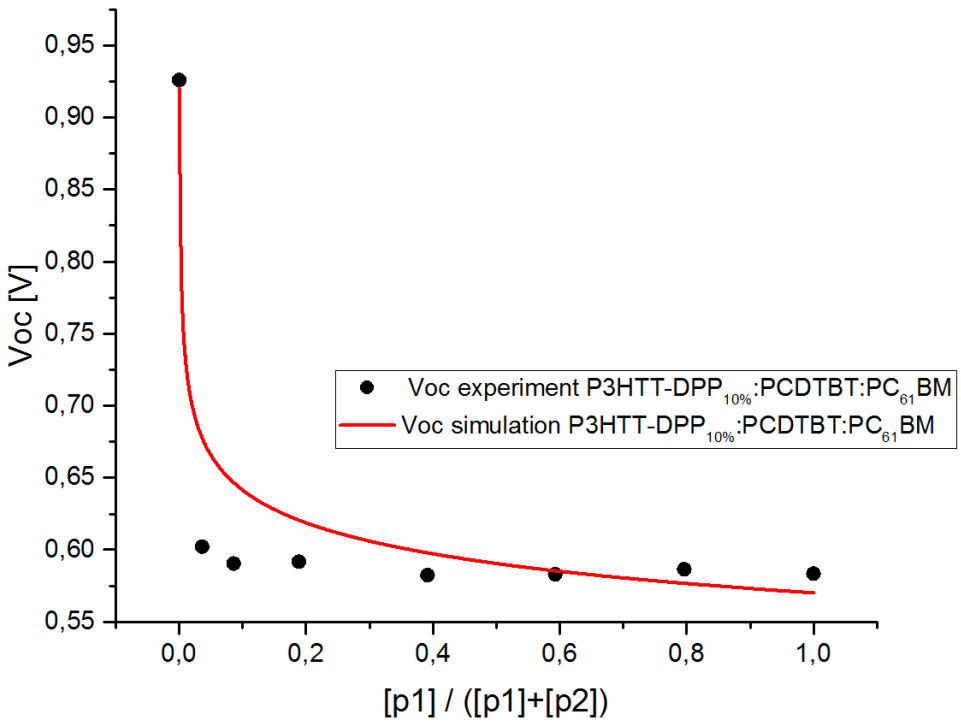

Fig. S6. Fitting of the P3HTT-DPP10%:PCDTBT:PC61BM ternary BHJ OPV from Khlyabich *et al.* [1] assuming constant occupation.

σ P3HTT-DPP10% [eV]	0.075
σ P3HTT-PCDTBT [eV]	0.075
σ PC61BM [eV]	0.075
occupation	$7.2 \cdot 10^{-4}$
total_Po_No	10^{26}
HOMO P3HTT-DPP10% [eV]	-5.25
HOMO PCDTBT [eV]	-5.6
LUMO PC61BM [eV]	-4.10

Table S3. Parameter values used in the simulation model for the fitting of the P3HTT-DPP10%:PCDTBT:PC61BM ternary BHJ OPV from Khlyabich *et al.* [1] assuming constant occupation.

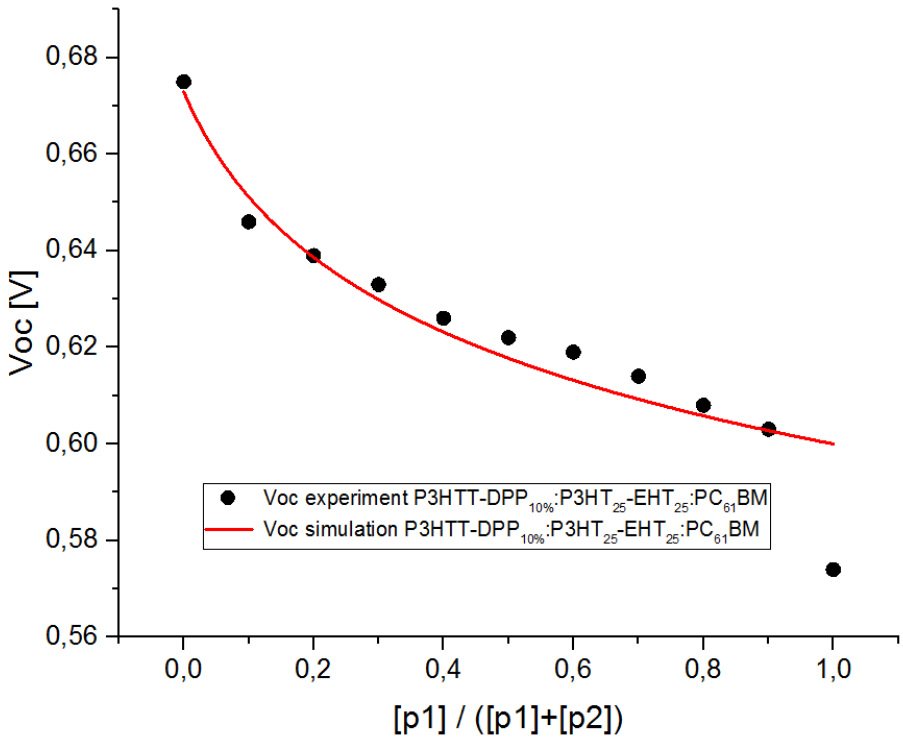

Fig. S7. Fitting of the P3HTT-DPP10%:P3HT25-EHT25:PC61BM ternary BHJ OPV from Khlyabich *et al.* [2] assuming constant occupation.

σ P3HTT-DPP10% [eV]	0.075
σ P3HT25-EHT25 [eV]	0.105
σ PC61BM [eV]	0.075
occupation	$1.2 \cdot 10^{-3}$
total_Po_No	10^{26}
HOMO P3HTT-DPP10% [eV]	-5.25
HOMO P3HT25-EHT25 [eV]	-5.40
LUMO PC61BM [eV]	-4.10

Table S4. Parameter values used in the simulation model for the fitting of P3HTT-DPP10%:P3HT25-EHT25:PC61BM from Khlyabich *et al.* [2] assuming constant occupation.

6 – Absorption spectra and parameters for Fig. 4

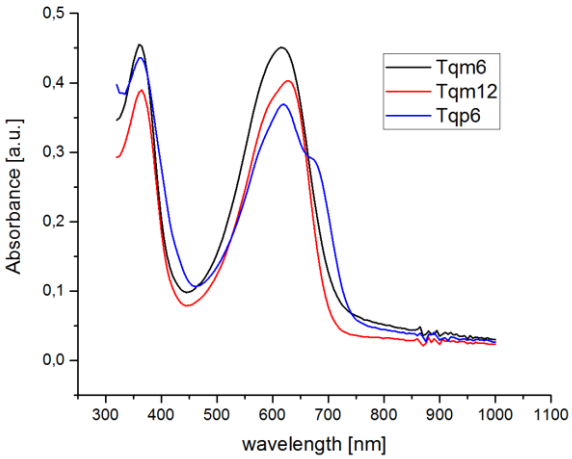

Fig. S8. UV-vis spectra of TQm6, TQm12 and TQp6 polymers. The FWHM were measured to be 148nm, 138nm and 175nm for TQm6, TQm12 and TQp6, respectively. Used films are ~80 nm thick, spin-coated on glass substrates.

σ_{TQm6} [eV]	0.1
σ_{TQm12} [eV]	0.09
σ_{PC71BM} [eV]	0.12
DOS	$5.5 \cdot 10^{26}$
$LUMO_{TQm6}$ [eV]	-3.80
$HOMO_{TQm6}$ [eV]	-5.72
$LUMO_{TQm12}$ [eV]	-3.45
$HOMO_{TQm12}$ [eV]	-5.76
$LUMO_{PC71BM}$ [eV]	-4.10
IQE	0.85
$lifetime_{holes}$ [s]	10^{-5}
$lifetime_{electrons}$ [s]	10^{-5}
FF	0.45
$FWHM_{TQm6}$ [m]	$148 \cdot 10^{-9}$
$FWHM_{TQm12}$ [m]	$138 \cdot 10^{-9}$
$Length_{Device}$ [m]	$100 \cdot 10^{-9}$
Abs. $length_{TQm6}$ [m]	$60 \cdot 10^{-9}$
Abs. $length_{TQm12}$ [m]	$95 \cdot 10^{-9}$

Table S5. Parameter values used in the simulation model for the fitting of the experimental Voc, Jsc and PCE data for TQm6:TQm12:$PC_{71}BM$ in Fig. 4. The $length_{device}$ corresponds to the mean thickness of the investigated device. As these devices are semi-transparent the device thickness corresponds to the optical path length.

7 – Performance indicators of TQp6:TQm6:$PC_{71}BM$ and TQp6:TQm12:$PC_{71}BM$

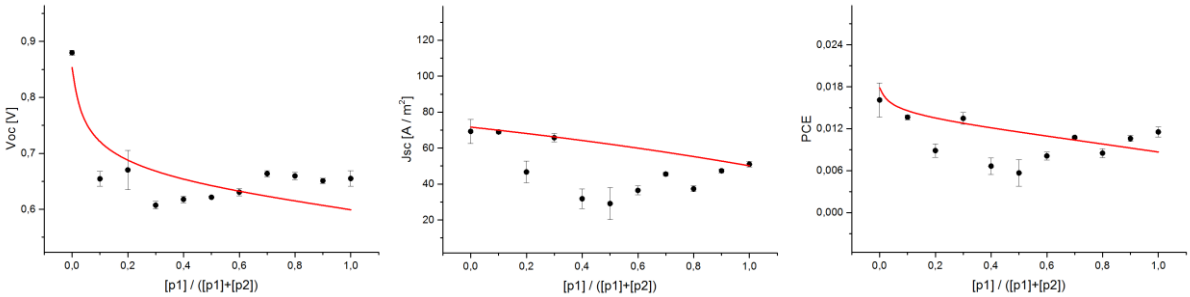

Fig. S9. Simulation of experimental Voc, Jsc, PCE data vs composition for the TQp6:TQm6:$PC_{71}BM$ ternary OPVs. Symbols and lines are experiments and simulations, respectively.

σ $_{TQp6}$ [eV]	0.12
σ $_{TQm6}$ [eV]	0.1
σ $_{PC71BM}$ [eV]	0.12
DOS	10^{26}
LUMO $_{TQp6}$ [eV]	-3.1
HOMO $_{TQp6}$ [eV]	-5.55
LUMO $_{TQm6}$ [eV]	-3.3
HOMO $_{TQm6}$ [eV]	-5.72
LUMO $_{PC71BM}$ [eV]	-4.1
IQE	0.85
lifetime$_{holes}$ [s]	10^{-5}
lifetime$_{electrons}$ [s]	10^{-5}
FF	0.3
FWHM $_{TQp6}$ [m]	$175 \cdot 10^{-9}$
FWHM $_{TQm6}$ [m]	$148 \cdot 10^{-9}$
Length $_{Device}$ [m]	$80 \cdot 10^{-9}$
Abs. length $_{TQp6}$ [m]	$120 \cdot 10^{-9}$
Abs. length $_{TQm6}$ [m]	$60 \cdot 10^{-9}$

Table S6. Parameter values used in the simulation model for the fitting of the experimental Voc, j_{SC} and PCE data for TQp6:TQm6:$PC_{71}BM$ (Fig. S7). The length$_{device}$ corresponds to the mean thickness of the investigated device. As these devices are semi-transparent the device thickness corresponds to the optical path length.

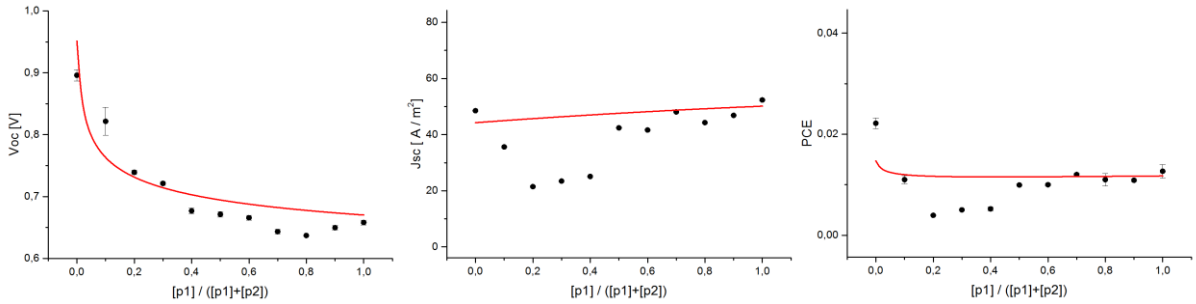

Fig. S10. Simulation of experimental Voc, j_{SC}, PCE data vs composition for the TQp6:TQm12:$PC_{71}BM$ ternary OPVs. Symbols and lines are experiments and simulations, respectively.

σ $_{TQp6}$ [eV]	0.12
σ $_{TQm12}$ [eV]	0.09
σ $_{PC71BM}$ [eV]	0.12
DOS	$3 \cdot 10^{25}$
LUMO $_{TQp6}$ [eV]	-3.1
HOMO $_{TQp6}$ [eV]	-5.55
LUMO $_{TQm12}$ [eV]	-3.15
HOMO $_{TQm12}$ [eV]	-5.76
LUMO $_{PC71BM}$ [eV]	-4.1
IQE	0.85
lifetime$_{holes}$ [s]	10^{-5}
lifetime$_{electrons}$ [s]	10^{-5}
FF	0.35
FWHM $_{TQp6}$ [m]	$175 \cdot 10^{-9}$
FWHM $_{TQm12}$ [m]	$138 \cdot 10^{-9}$
Length $_{Device}$ [m]	$80 \cdot 10^{-9}$
Abs. length $_{TQp6}$ [m]	$120 \cdot 10^{-9}$
Abs. length $_{TQm12}$ [m]	$95 \cdot 10^{-9}$

Table S7. Parameter values used in the simulation model for the fitting of the experimental Voc, Jsc and PCE data for TQp6:TQm12:$PC_{71}BM$ (Fig. S8). The $length_{device}$ corresponds to the mean thickness of the investigated device. As these devices are semi-transparent the device thickness corresponds to the optical path length.

8 – Method for finding the optimal composition

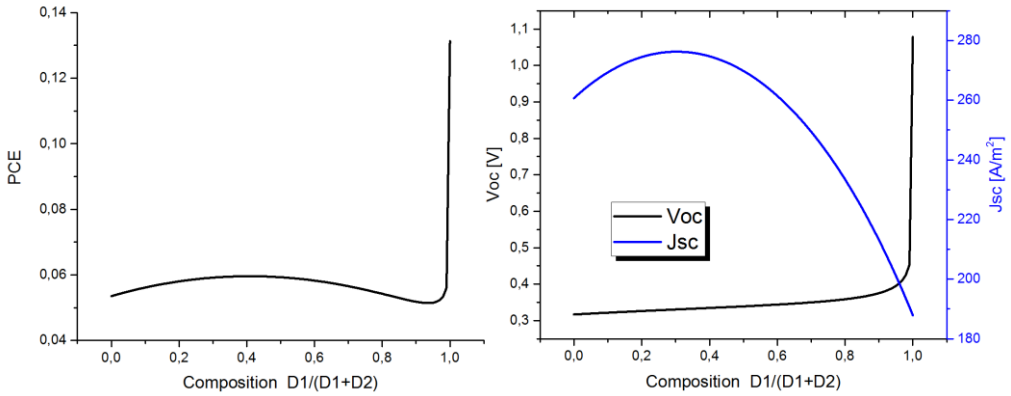

Fig. S11. (left) PCE vs composition plot for the D1, D2 pair that gives the highest overall PCE in Fig. 6. The optimal composition that gives the best PCE is in this case 100% of D1, D1/(D1+D2) = 1, i.e. a pure binary system. The sudden jumps in optimal composition observed in Figs. 6, 7 that do not sit at the binary line (y=x) are associated with the presence of two local maxima in this curve. At the discontinuity the dominant maximum changes from ternary to binary or vice versa. (right) Corresponding Voc and j_{SC}.

9 – Parameters values for Figs. 5, 6, 7 and 8

σ $_{\text{Donor1}}$ [eV]	0.075
σ $_{\text{Donor2}}$ [eV]	0.075
σ $_{\text{Acceptor}}$ [eV]	0.075
DOS	10^{26}
HOMO $_{\text{Donor1}}$ [eV]	-5.4
LUMO $_{\text{Donor1}}$ [eV]	-2.5 … -4.1
HOMO $_{\text{Donor2}}$ [eV]	-5.4
LUMO $_{\text{Donor2}}$ [eV]	-2.5 … -4.1
LUMO $_{\text{Acceptor}}$ [eV]	-4.1
IQE	0.85
lifetime$_{\text{holes}}$ [s]	10^{-5}
lifetime$_{\text{electrons}}$ [s]	10^{-5}
FF	0.65
FWHM $_{\text{Donor1}}$ [m]	$175 \cdot 10^{-9}$
FWHM $_{\text{Donor2}}$ [m]	$175 \cdot 10^{-9}$
Length $_{\text{Device}}$ [m]	$240 \cdot 10^{-9}$
Abs. length $_{\text{Donor1}}$ [m]	$120 \cdot 10^{-9}$
Abs. length $_{\text{Donor2}}$ [m]	$120 \cdot 10^{-9}$

Table S8. Parameter values used for the LUMO variation simulations in Fig. 5, inspired by the work of Yang *et al*. (Ref. [3]). The length$_{\text{device}}$ corresponds to two times the actual device thickness to account for the fact that the optical path length (in lowest order) is twice the device thickness in devices with a reflective back electrode. For Figs. 6, 7 and 8 the same parameters are used, except (a) the HOMO levels that are varied, fixing the (common) LUMO level at -3.8 eV; (b) the absorption spectra are calculated on an energy axis, using FWHM = 0.80 eV (for Fig. 6) or FWHM = 0.50 eV (for Fig. 7) for both D1 and D2 and (c) for Fig. 8 the fill factor was not constant but given by $FF(f_{D1}) = af_{D1}^2 + (FF_{D1} - FF_{D2} - a)f_{D1} + FF_{D2}$.

10 – Applying the model to binary OPV

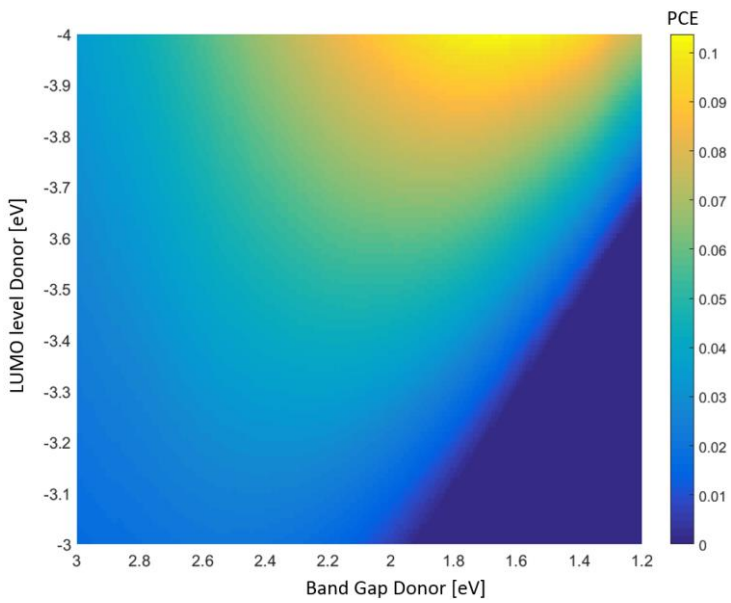

Fig. S12. PCE vs Donor LUMO-HOMO level for binary devices, reproducing the work of Scharber *et al*.[4]

σ $_{\text{Donor}}$ [eV]	0.075
σ $_{\text{Acceptor}}$ [eV]	0.075
DOS	10^{26}
Gap $_{\text{Donor}}$ [eV]	1.2 … 3.0
LUMO $_{\text{Donor}}$ [eV]	-3.0 … -4.0
LUMO $_{\text{Acceptor}}$ [eV]	-4.3
IQE	0.85
lifetime$_{\text{holes}}$ [s]	10^{-5}
lifetime$_{\text{electrons}}$ [s]	10^{-5}
FF	0.65
Length $_{\text{Device}}$ [m]	$240 \cdot 10^{-9}$
Abs. length $_{\text{Donor1}}$ [m]	$60 \cdot 10^{-9}$

Table S9. Parameter values used for reproducing the work of Scharber *et al*.[3] Following Ref. [3], the polymers absorption profile is taken as a step function. The length$_{\text{device}}$ corresponds to two times the actual device thickness to account for the fact that the optical path length (in lowest order) is twice the device thickness in devices with a reflective back electrode. The IQE value of 0.85 differs from the 0.65 used by Scharber *et al*. and compensates for the fact that our (more advanced) definition of Voc leads to lower Voc values.

11 – More ternary systems

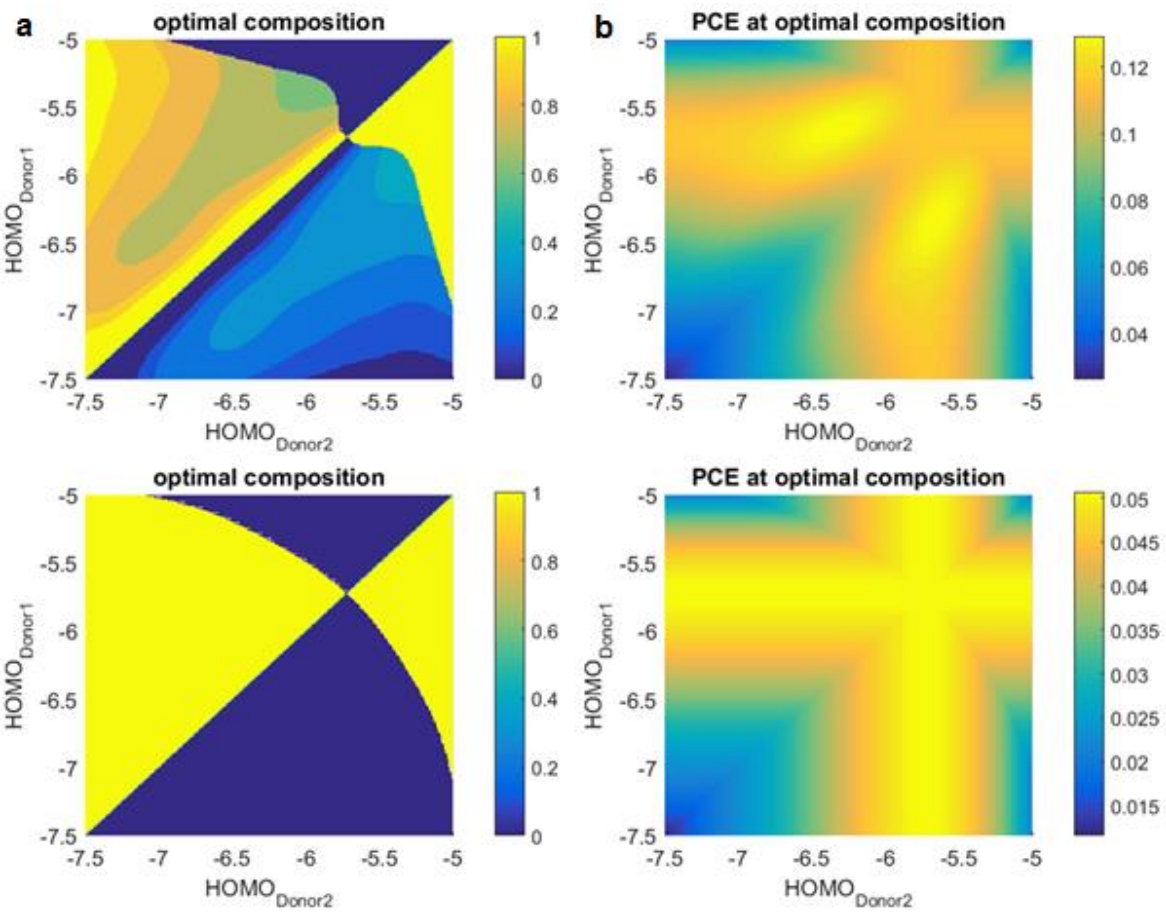

Fig. S13. (a) Optimal fraction of Donor 1 and (b) associated PCE for all different HOMO level combinations for a narrower absorber (FWHM = 0.5 eV) of high (top, L_D = 50 nm) and low (bottom, L_D = 240 nm) absorption strength; the LUMO level is fixed at -3.8 eV, the optical path length is 240 nm. The other parameters are as in Table T7 and Figs. 5,6,7. The images illustrate that narrow but strong absorbers give rise to systems where ternary compositions offer improved performance over binary ones whereas a weaker absorption shifts the balance to binary-dominated ones.

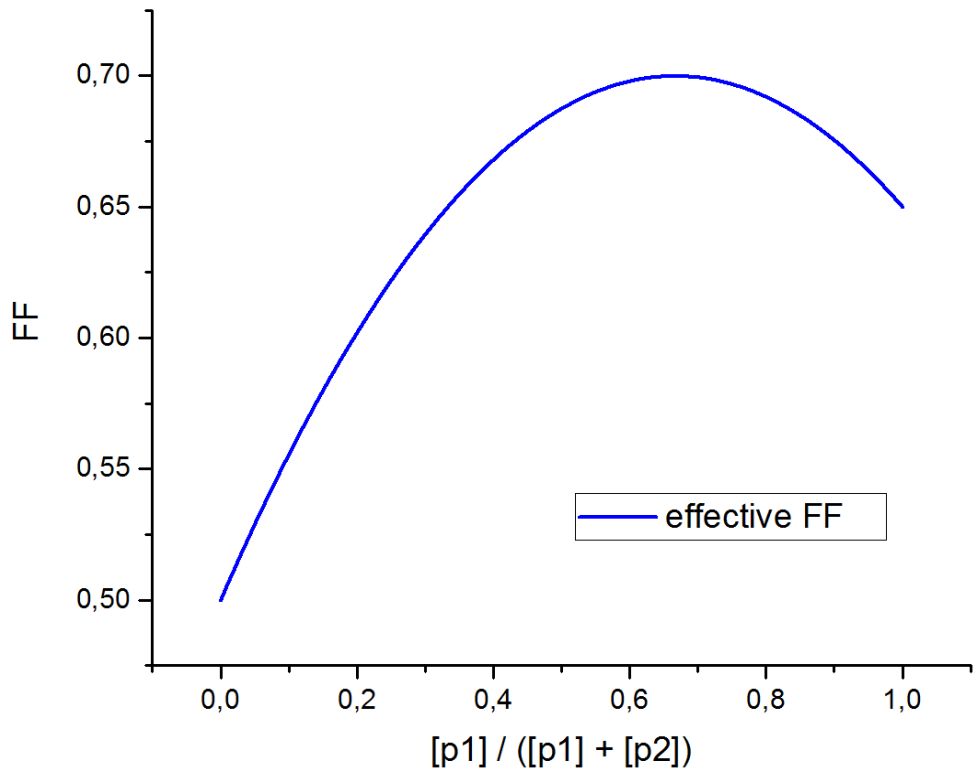

Fig. S14. Effective FF for FF_{Donor1} = 0.65 , FF_{Donor2} = 0.5 and α = -0.45. The FF is asymmetric with respect to donor composition due to the unequal FF at the binary extremities and reaches a maximum of 0.70 at 66% Donor1/ (Donor1+Donor2) composition.

References

[1] P. P. Khlyabich , Andrey E. Rudenko , Barry C. Thompson , and Yueh-Lin Loo, *Adv. Funct. Mater.* **2015**, 25, 5557–5563

[2] P. P. Khlyabich, B. Burkhart, B. C. Thompson, *J. Am. Chem. Soc.* **2012**, *134*, 9074.

[3] Y. (Michael) Yang, W. Chen, L. Dou, W.-H. Chang, H.-S. Duan, B. Bob, G. Li, Y. Yang, *Nat. Photonics* **2015**, *advance online publication*, DOI 10.1038/nphoton.2015.9.

[4] M. C. Scharber, D. Mühlbacher, M. Koppe, P. Denk, C. Waldauf, A. J. Heeger, C. J. Brabec, *Adv. Mater.* **2006**, *18*, 789.